Out-of-band spectral correction algorithm for the Multi-angle Imaging Spectro-Radiometer

Nadine Chrien, Carol **Bruegge**

Jet Propulsion Laboratory, California Institute of Technology
4S00 Oak Grove Drive, **Pasadena,** California 91109

AIMTRACT

An out-of-band correction algorithm is evaluated for the Multi-angle Imaging **Spectro-Radiometer (MISR).** The objective for MISR is to report scene **radiances, as averaged** over the in-band spectral response region. This product does not follow **directly** from the **radiometric** calibration process, which is sensitive to the out-of-band scene content. In-order to provide a correction, a retrieval of the scene spectral **profile** is **needed.** For MISR this can only be done **within** the four bands (nominally 443, 555,670, and 865 rim). Data which includes a continuum of scene wavelengths arc provided by using imagery from the Airborne Visible/ Infrared Imaging **Spectrometer (AVIRIS). These** data are used hereto evaluate the **proposed** out-of-band **correction** algorithm. This study shows that there can be as large as a 4% **difference** in the total band-weighted spectral radiance, as compared to the desired in-band weighted spectral radiance. The proposed algorithm provides the desired product, to within 0.5% accuracy.

KEYWORD LIST

Spectral calibration, EOS, MISR

1. INTRODUCTION

The **Earth** Observing System **(EOS)/** Multi-angle Imaging Spcctro-Radiometer **(MISR)** instrument has spectral calibration **requirements** that include **centroid** knowledge to within 0.5 nrn, uniformity of spectral center wavelength and bandwidth to within 2.0 nm or **less** (band dependent), and mission life stability to within 1 nm. **Recently** the nine cameras have **completed** calibration and characterization testing. With these as-built performance data in-hand, the science team is now in a position **to** define procedures for producing the **radiometric** and scientific products. The current plans call for Level 1 **processing** that will:

- usc **radiometric** calibration coefficients to scale camera digital numbers **(DN)** to spectral radiances, reported in MKS *(meter,* kilogram, second) units referred to as S1 **(Système** International);
- report these **spectral** radiances band-weighted over the entire response range of the **sensor;**
- usc the preflight measured point-spread-function **(PSF)** responses, in conjunction with image restoration techniques, to provide a contrast enhancement to the data;
- use **solar-irradiance** scaling factors to convert the radiances to a common in-band response function; and
- provide registration, for images from the nine cameras, and Earth **georectification.**

During **pre-flight** testing, it was **discovered** that the **out-of-band** spectral **rejection** does not meet the instrument **specification** requirements. This is believed to be due primarily to scattering centers within the filters causing a **certain** fraction of **the** light to transit the filters at sufficiently oblique angles relative to normal incidence such that the interference filters enable **out**-of-band **light** to be transmittal'. For scenes with the same spectral signature as the target used in calibration of **the** MISR **cameras** *(i.e.,* **the** on-board **Spectralon** panels), this out-of-band light **results** in no **radiometric** error. However, for **scenes** of different spectral content, small **radiometric** errors result from the fact that the out-of-band integrated response is typically about **3%** of the integrated in-band response. Thus, a **correction** for this phenomenon is desirable **as well.** However, this *correction* requires **co-registration** of the four MISR bands in order to obtain an estimate of the **scene** spectrum, and this registration is not available during Level **1B** 1 processing due to the spatial displacement of the **spectral** bands within the camera focal planes. This registration is **effected** during higher **level** processing, once the altitude of the scene is determined. Because the out-of-band **correction** may not **be** desired by all geophysical retrieval algorithms, implementation of this step is **deferred** to those Level 2 processes that require it.

This paper **evaluates** the proposed Level 2 out-of-band correction algorithm for **MISR.**

2. MATHEMATICAL DESCRII'TIONS

For each spectral band, the in-band region is defined to be that continuous wavelength range which includes the wavelength of the peak system response, and for which the system transmittance is consistentl y greater than 1 % of the peak system response. The wavelength region outside this range is referred to as out-of-band. A method for correcting the measured radiance to account for unwanted out-of-band contributions is to estimate the out-of-band radiance measured for a particular scene by utilizing the retrieved reflectance from the other MISR bands for that scene. This estimated out-of-band radiance is then subtracted from the total measured radiance to produce a corrected estimate of the in-band weighted radiance.

The measured band-weighted radiance L_λ is defined in Equation 1 for a MISR band represented by wavelength λ, where λ is nominally 443 nm, 555 nm, 670 nm, and 865 nm for the four MISR bands also referred to as Bands 1,2.3. and 4. $L_{\lambda'}$ represents the spectral radiance of an observed terrestrial scene, and $\Re_{\lambda,\lambda'}$ represents the measured camera spectral response. The term *total* indicate-s that the integration is over all wavelengths to which the MISR cameras respond, nominally 365 nm to 1150 nm.

$$L_\lambda = \frac{\int_{\text{total}} L_{\lambda'} \Re_{\lambda,\lambda'} \lambda' d\lambda'}{\int_{\text{total}} \Re_{\lambda,\lambda'} \lambda' d\lambda'} \tag{1}$$

The actual in-band weighted radiance and actual in-band weighted equivalent reflectance are expressed in Equations 2 and 3 where $E_{o\lambda'}$ represents the solar spectral irradiance. This is the radiance that would ideally be measured.

$$L_{\text{AIB},\lambda} = \frac{\int_{\text{in-band}} L_{\lambda'} \Re_{\lambda,\lambda'} \lambda' d\lambda'}{\int_{\text{in-band}} \Re_{\lambda,\lambda'} \lambda' d\lambda'} \tag{2}$$

$$\rho_{\text{AIB},\lambda} = \frac{\pi \int_{\text{in-band}} L_{\lambda'} \Re_{\lambda,\lambda'} \lambda' d\lambda'}{\int_{\text{in-band}} E_{o,\lambda'} \Re_{\lambda,\lambda'} \lambda' d\lambda'} \tag{3}$$

As part of the Level1B1[1] processing, the radiometrically calibrated output of each pixel within a given band, for all cameras, is transformed to a standard in-band spectral response function. In this manner, a single standard response function can be used to characterize each pixel of each camera of a particular MISR band. The camera spectral response functions and standardized in-band response functions used in this study are shown in Figure 1, The out-of-band integrated response is 1.4%, 2.8940, 2.8%, and 2.7% of the integrated in-band response for Bands 1,2,3, and 4 respectively.

Let $S_{\lambda,\lambda'}$ represent the standardized camera spectral response for Band λ, then the standardized band-weighted radiance is defined in Equation 4, and the retrieved band-weighted equivalent reflectance for Band, λ is given by Equation 5.

$$L_\lambda^{corr} = L_\lambda \cdot \frac{\int_{\text{total}} E_{o,\lambda'} S_{\lambda,\lambda'} \lambda' d\lambda'}{\int_{\text{total}} S_{\lambda,\lambda'} \lambda' d\lambda'} + \frac{\int_{\text{total}} E_{o,\lambda'} \Re_{\lambda,\lambda'} \lambda' d\lambda'}{\int_{\text{total}} \Re_{\lambda,\lambda'} \lambda' d\lambda'} \tag{4}$$

$$\rho_{S,\lambda} = \pi L_\lambda^{corr} \cdot \frac{\int_{total} S_{\lambda,\lambda'} \lambda' d\lambda'}{\int_{total} E_{o,\lambda'} S_{\lambda,\lambda'} \lambda' d\lambda'} \tag{5}$$

The band-weighted equivalent reflectance for a particular observed scene from each of the four MISR bands will provide four samples of the scene spectral equivalent reflectance over the wavelength range spanned by MISR. From this sample we can estimate the scene spectral equivalent reflectance; when combined with our knowledge of the MISR standard spectral response for each band and a model of the exe-atmospheric solar spectral irradiance[2], wc can estimate the out-of-band radiance in the observed scene.

Let $\rho'_{S\lambda'}$ denote the scene spectral equivalent reflectance. It is derived from a piecewise linear interpolation of the band-weighted equivalent reflectances, $\rho_{S,\lambda}$, as shown in Equation 7. The estimated out-of-band radiance in the observed scene is then found to be

$$L_{EOB,\lambda} = \int_{\text{out-of-band}} \rho'_{S,\lambda'} E_{o,\lambda'} S_{\lambda,\lambda'} \lambda' d\lambda' \tag{6}$$

for the MISR band denoted by λ.

$$\rho'_{S,\lambda'} = \begin{cases} \rho_{S,B1}, & \lambda' \le \lambda_{c,B1} \\ \left[\frac{(\rho_{S,B2}-\rho_{S,B1})}{(\lambda_{c,B2}-\lambda_{c,B1})} \cdot \lambda' + \frac{(\rho_{S,B1}\lambda_{c,B2}-\rho_{S,B2}\lambda_{c,B1})}{(\lambda_{c,B2}-\lambda_{c,B1})}\right], & \lambda_{c,B1} < \lambda' \le \lambda_{c,B2} \\ \left[\frac{(\rho_{S,B3}-\rho_{S,B2})}{(\lambda_{c,B3}-\lambda_{c,B2})} \cdot \lambda' + \frac{(\rho_{S,B2}\lambda_{c,B3}-\rho_{S,B3}\lambda_{c,B2})}{(\lambda_{c,B3}-\lambda_{c,B2})}\right], & \lambda_{c,B2} < \lambda' < \lambda_{c,B3} \\ \left[\frac{(\rho_{S,B4}-\rho_{S,B3})}{(\lambda_{c,B4}-\lambda_{c,B3})} \cdot \lambda' + \frac{(\rho_{S,B3}\lambda_{c,B4}-\rho_{S,B4}\lambda_{c,B3})}{(\lambda_{c,B4}-\lambda_{c,B3})}\right], & \lambda_{c,3} < \lambda' < \lambda_{c,B4} \\ \rho_{S,B4}, & \lambda' > \lambda_{c,B4} \end{cases} \tag{7}$$

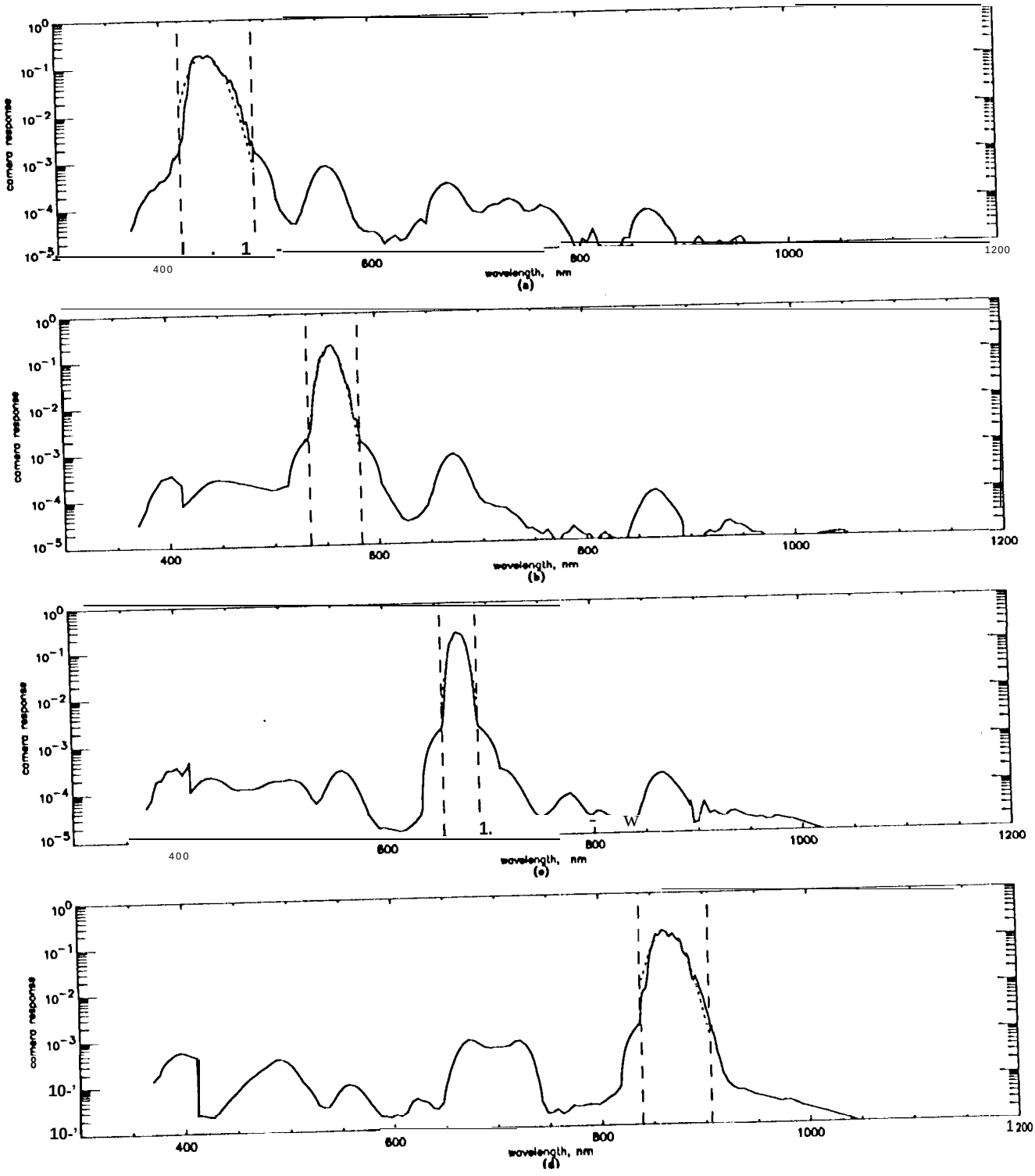

Figure 1. Measured camera spectral response for (a) Band 1, (b) Band 2, (c) Band 3, and (d) Band 4 (PFA244, on-axis) in-band region and standardized response denoted by dashed and doued lines.

A spectral correction to the measured band-weighted radiance may now be performed and an estimated in-band weighted radiance derived as in Equation 8. This may also be couched in terms of equivalent reflectance as expressed in Equation 9.

$$L_{\mathrm{EIB},\lambda} = \frac{L_{\lambda}^{corr} \cdot \int_{\text{total}} S_{\lambda,\lambda'}\lambda' d\lambda' - L_{\mathrm{EOB},\lambda}}{\int_{\text{in-band}} S_{\lambda,\lambda'}\lambda' d\lambda'} \tag{8}$$

$$\rho_{\mathrm{EIB},\lambda} = \frac{\pi L_{\mathrm{EIB},\lambda}}{\left(\int_{\text{in-band}} E_{o,\lambda'} S_{\lambda,\lambda'}\lambda' d\lambda'\right) / \left(\int_{\text{in-band}} S_{\lambda,\lambda'}\lambda' d\lambda'\right)} \tag{9}$$

The error in band-weighted radiance with no spectral correction applied is defined in Equation 10. The error in band-weighted radiance after the spectral correction is applied is found by substituting $L_{\mathrm{EIB},\lambda}$ for L_{λ}.

$$\varepsilon = \frac{(L_{\lambda} - L_{\mathrm{AIB},\lambda})}{L_{\mathrm{AIB},\lambda}} \tag{10}$$

The error in terms of band-weighted equivalent reflectance with no spectral correction applied is defined in Equation 11. The error after the spectral correction is applied is found by substituting $\rho_{\mathrm{EIB},\lambda}$ for $\rho_{S,\lambda}$.

$$\varepsilon_{\rho} = \frac{(\rho_{S,\lambda} - \rho_{\mathrm{AIB},\lambda})}{\rho_{\mathrm{AIB},\lambda}} \tag{11}$$

3. RESULTS

Spectral radiance data from the Airborne Visible/Infrared Imaging Spectrometer (AVIRIS)[3] were used to provide scene types for this study. Two cases arc presented here. In the first case, discrete spectra were chosen and the scene types identified visually from the image and knowledge of the site. To this set of scene types an ideal 100% equivalent reflectance spectrally flat data set was added. Also, added was spectral radiance for an AVIRIS field target (Spectralon™) based on measured spectral reflectance data and the exe-atmospheric solar irradiance model, In the second ease, all spatial elements of an AVIRIS image were examined.

3.1 Discrete scene types

Fourteen discrete scene types were selected for the first part of this study. They arc listed in Figure 2. The first ten were chosen from the AVIRIS image used in the second ease (Figure 8) to provide a varied sampling. Those scene types prefaced by the term *Mean are* represent by the mean spectral radiance over 14x 14 AVIRIS spatial elements. Since the ground instantaneous field-of-view of AVIRIS is 20 m, a 14 x 14 sample represents approximately one MISR pixel. The spectral radiance data from the AVIRIS imagery was converted to equivalent reflectance? (Figure 2) for comparison to the MISR band-weighted equivalent reflectance (Figure 3). It was AVIRIS radiance data directly that was used for the scene spectral radiance Lx.

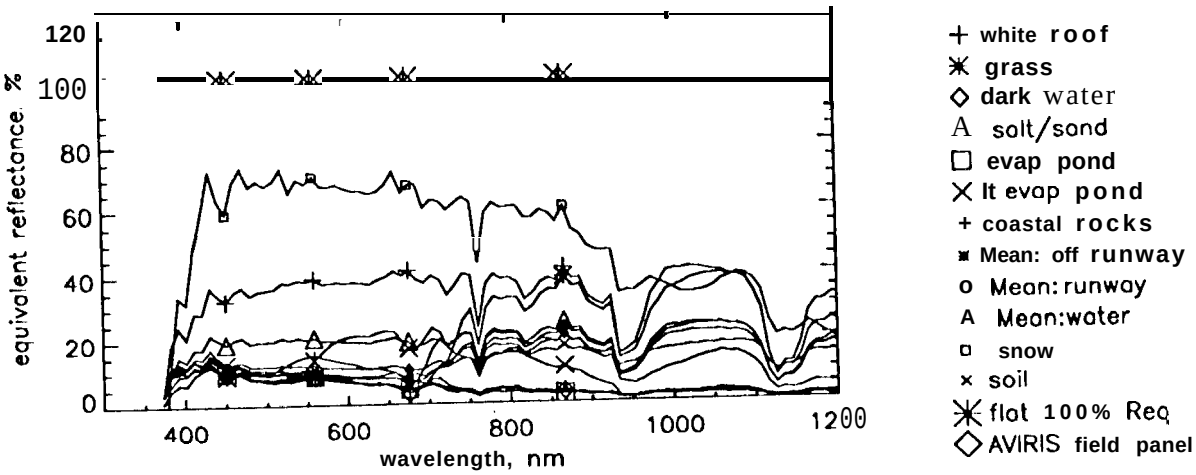

Figure 2. Scene types, equivalent reflectance versus wavelength

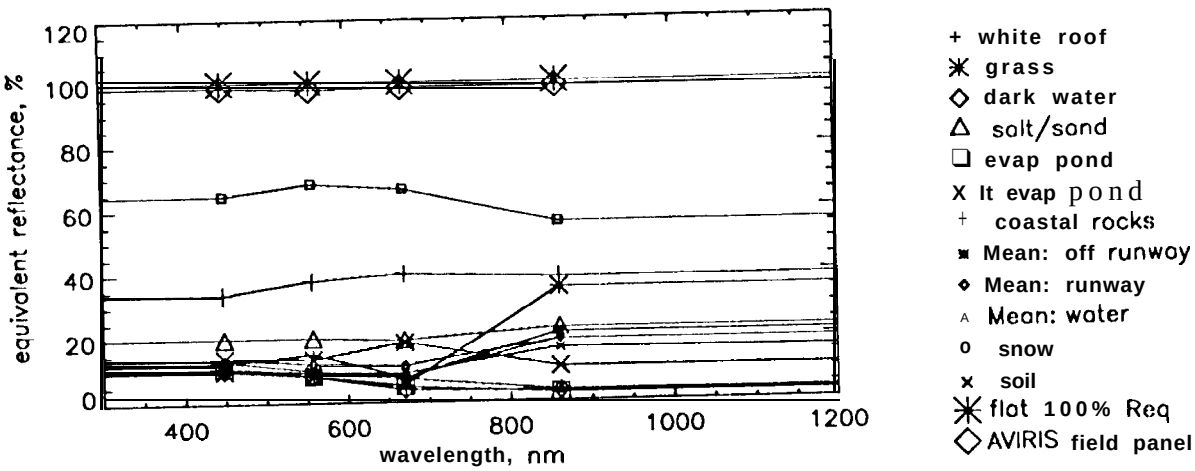

Figure 3. MISR band-weighted reflectance from observed scene types

The largest errors are found in scene types with low equivalent reflectance in-band. For score types with high equivalent reflectance or which are spectrall y rather flat, such as the white *roof, snow, AVIRIS field panel, flat 100% R_{eq}* scenes, there is little improvement seen with the spectral correction. In fact, in reflectance terms there is little to no error (in the case of the *flat 100% R_{eq}* scene) with or without correction. The error in radiance terms is due to the difference in the band-weighted solar spectral irradiance when in-band versus total integration limits are used.

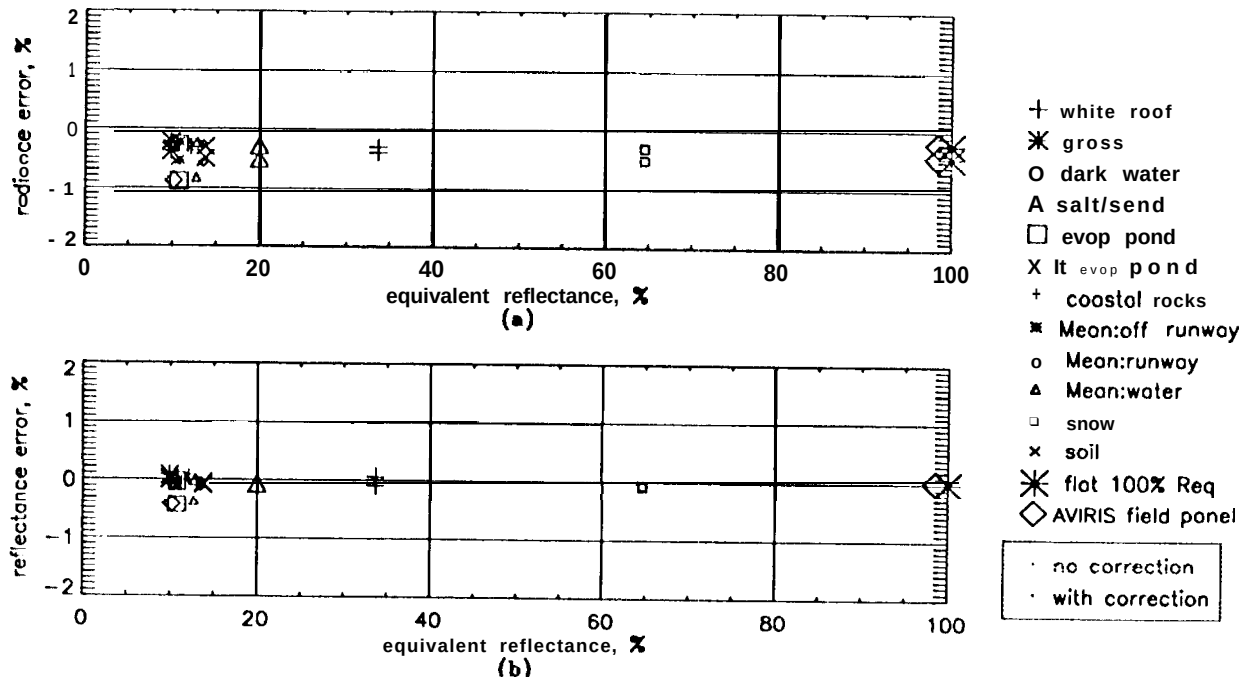

Figure 4. Band 1, error in (a) predicted radiance and (b) predicted equivalent reflectance

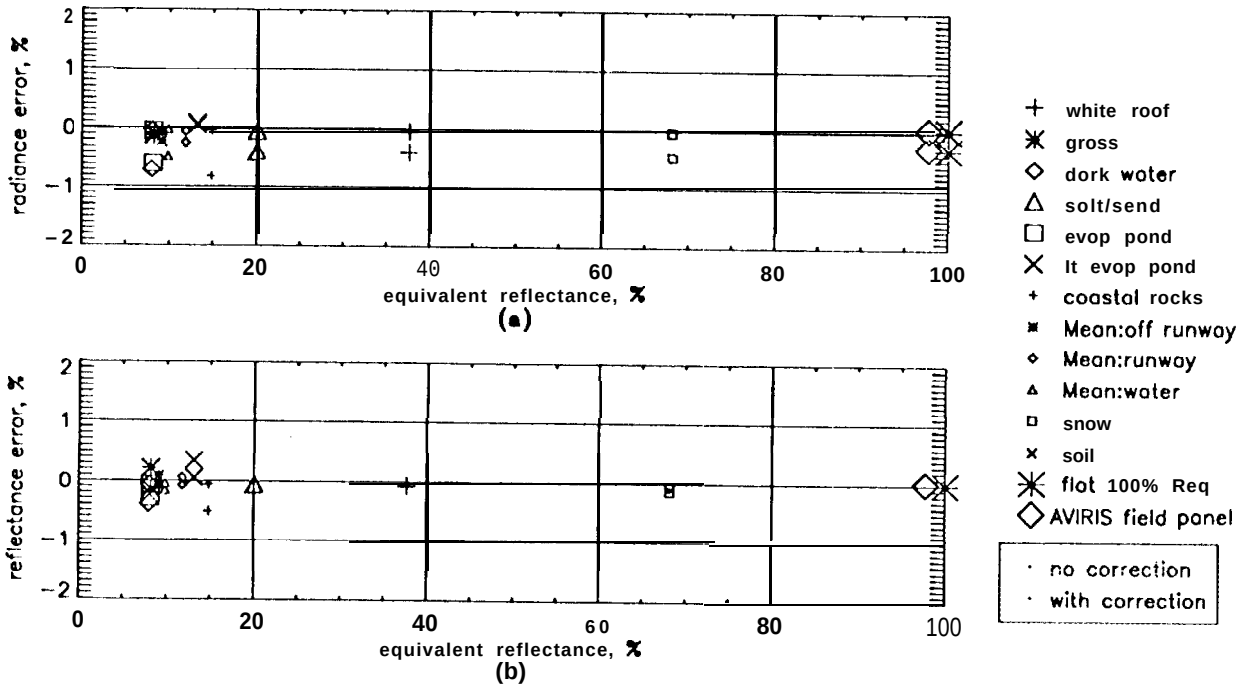

Figure 5. Band 2, error in (a) predicted radiance and (b) predicted equivalent reflectance

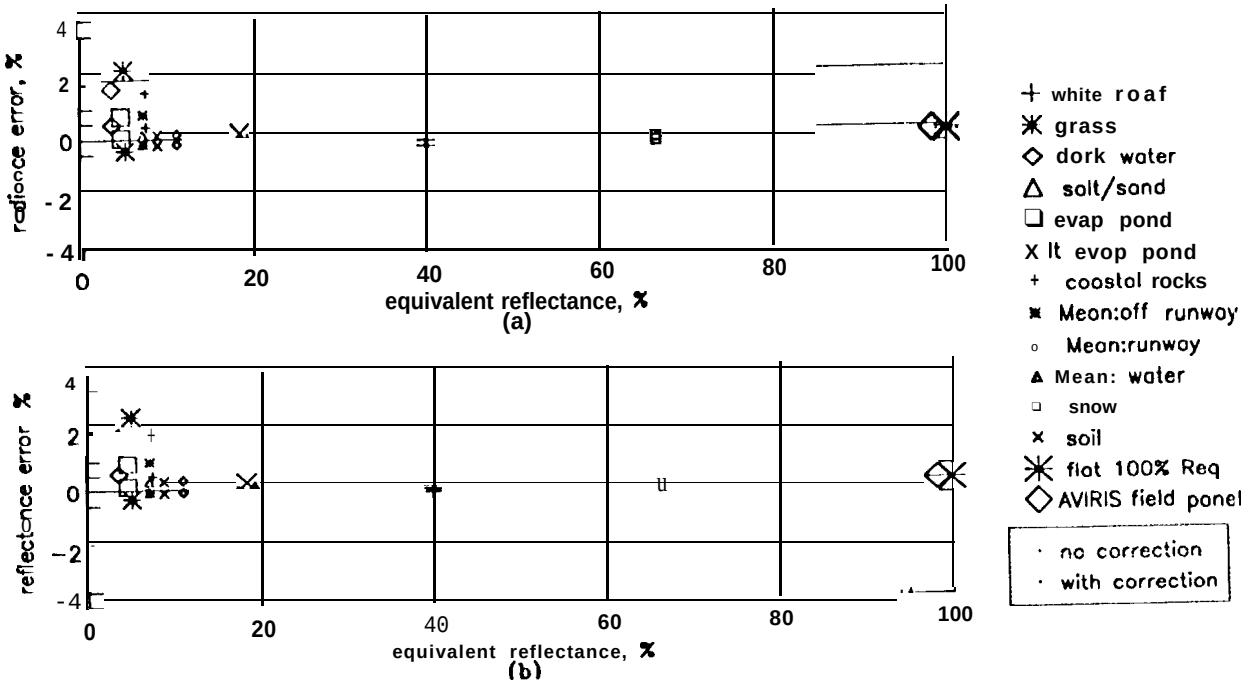

Figure 6. Band 3, error in (a) predicted radiance and (b) predicted equivalent reflectance

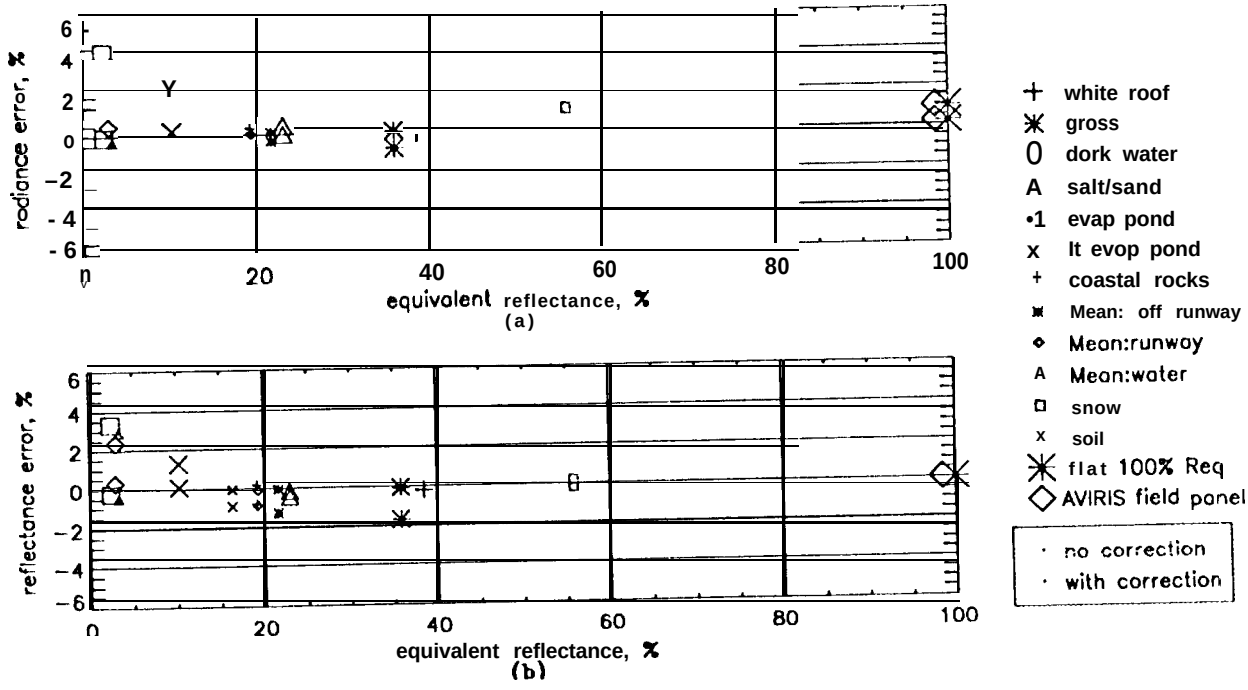

Figure 7. Band 4, error in (a) predicted radiance and (b) predicted equivalent reflectance

3.2Entire AVIRIS image

Figure 8. AVIRIS image of Moffett Field, California used in study from April 1994

The spectral radiance data, Lx, from each of the 614x512 spatial elements in the AVIRIS image shown in Figure 8 was used to model the MISR band-weighted radiance and the actual in-band weighted radiance for each of the four MISR spectral bands observed from each of the spatial elements. From these L_{λ} and $L_{AIB,\lambda}$, the spectral correction was applied and the error in terms of band-weighted equivalent reflectance was computed. These results are illustrated in Figures 9 through 12..

In Figures 9a, lOa, 1 la, and 12a, we see that without correction the low equivalent reflectance scenes show errors of up to 5% in Band 4. Band 1 shows the smallest errors, but it also had the best out-of-band rejection. In all bands it is the low equivalent reflectance scenes that show the largest radiometric errors.

After the spectral correction, the estimated in-band weighted equivalent reflectance shows improvement, and at low equivalent reflectances the errors are down to ±1 % for all bands.

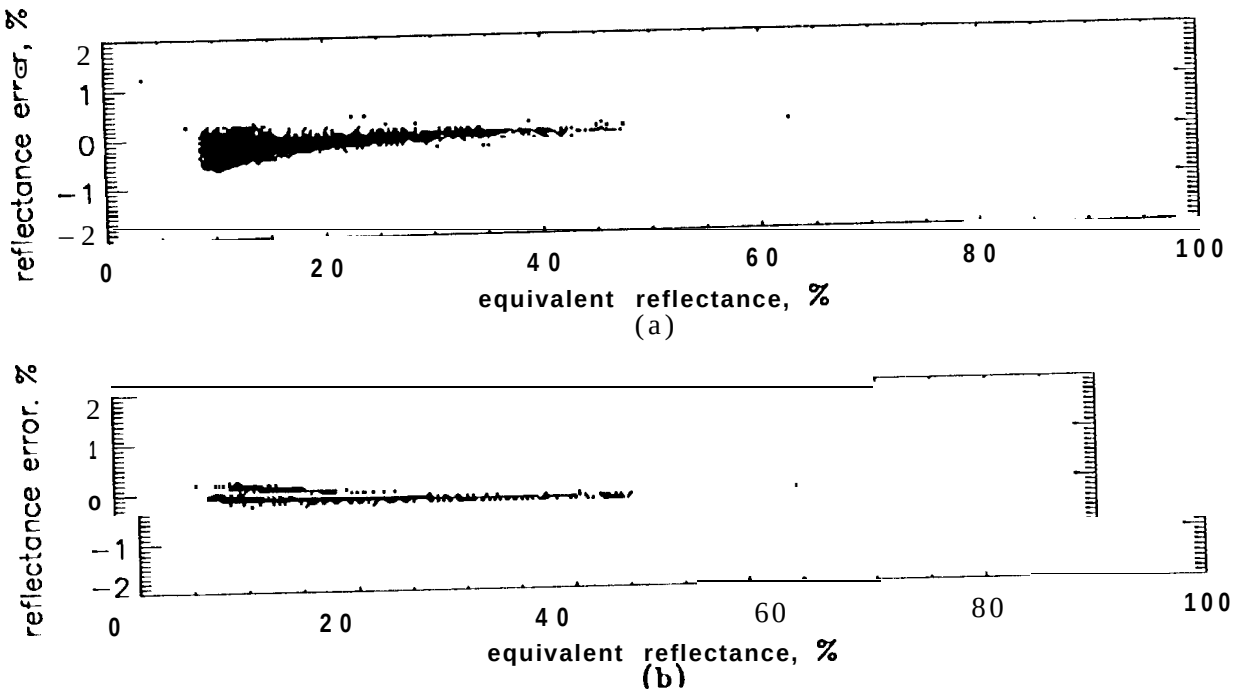

Figure 9. Band 1, errors in reflectance (a) without correction and (b) with out-of-band spectral correction.

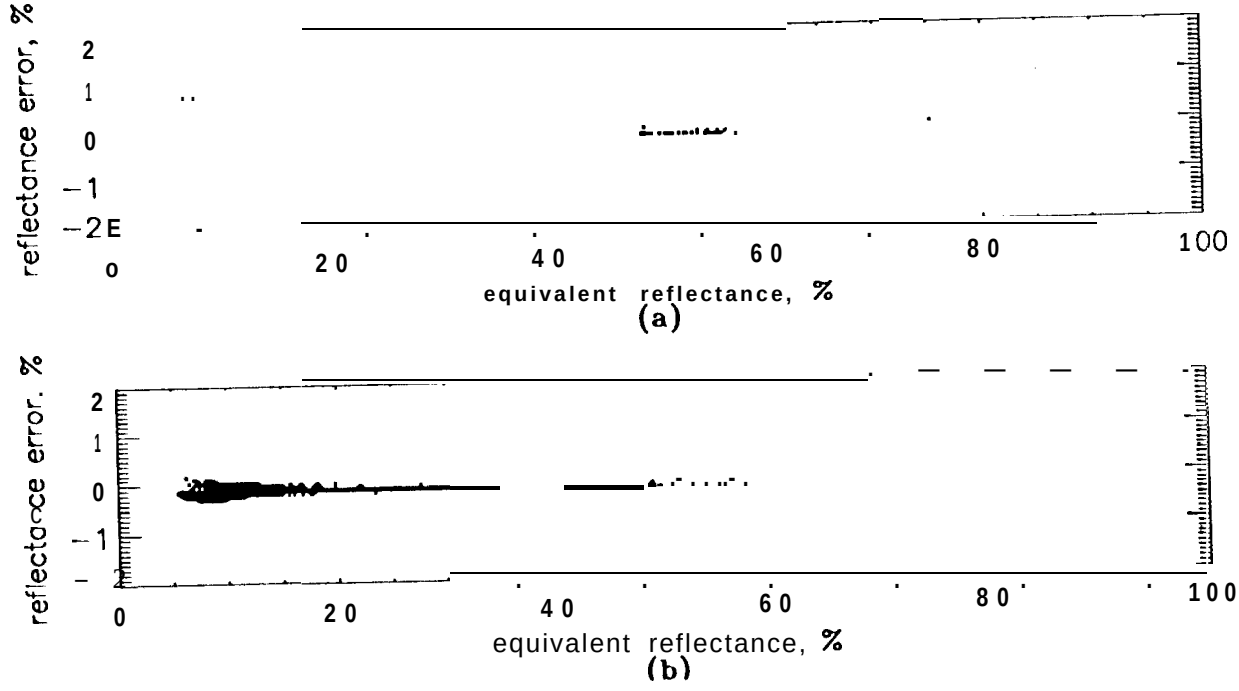

Figure 10. Band 2, errors in reflectance (a) without correction and (b) with out-of-band spectral correction.

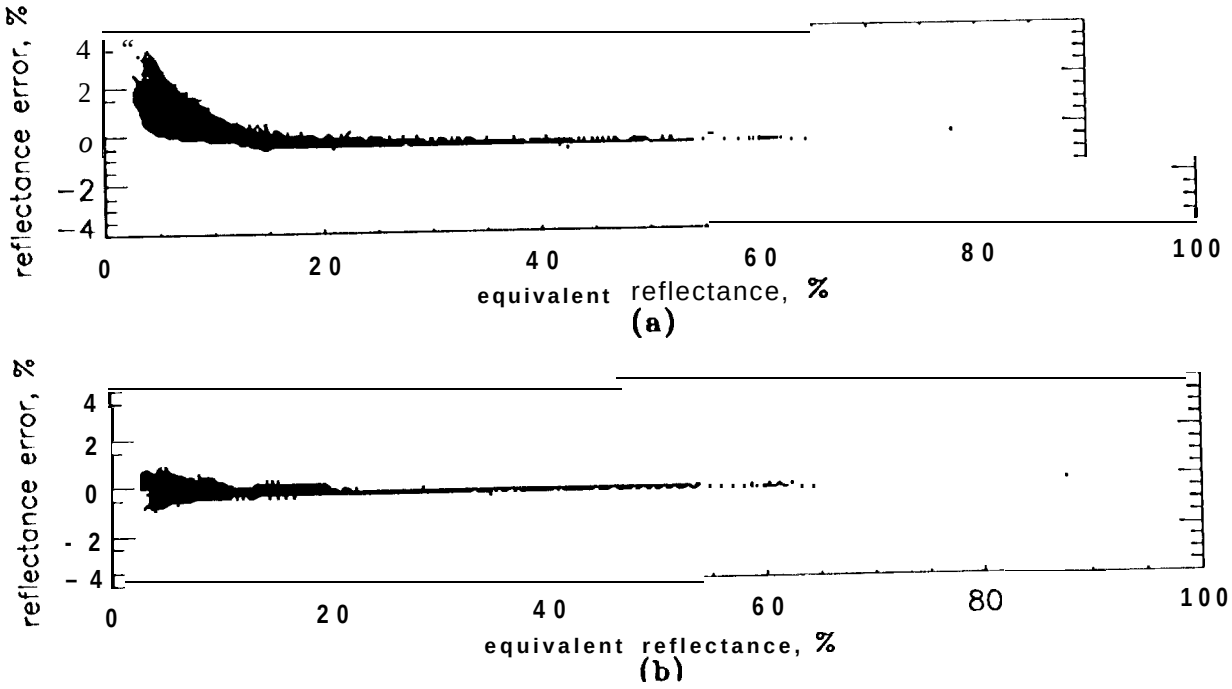

Figure 11. Band 3, errors in reflectance (a) without correction and (b) with out-of-band spectral correction.

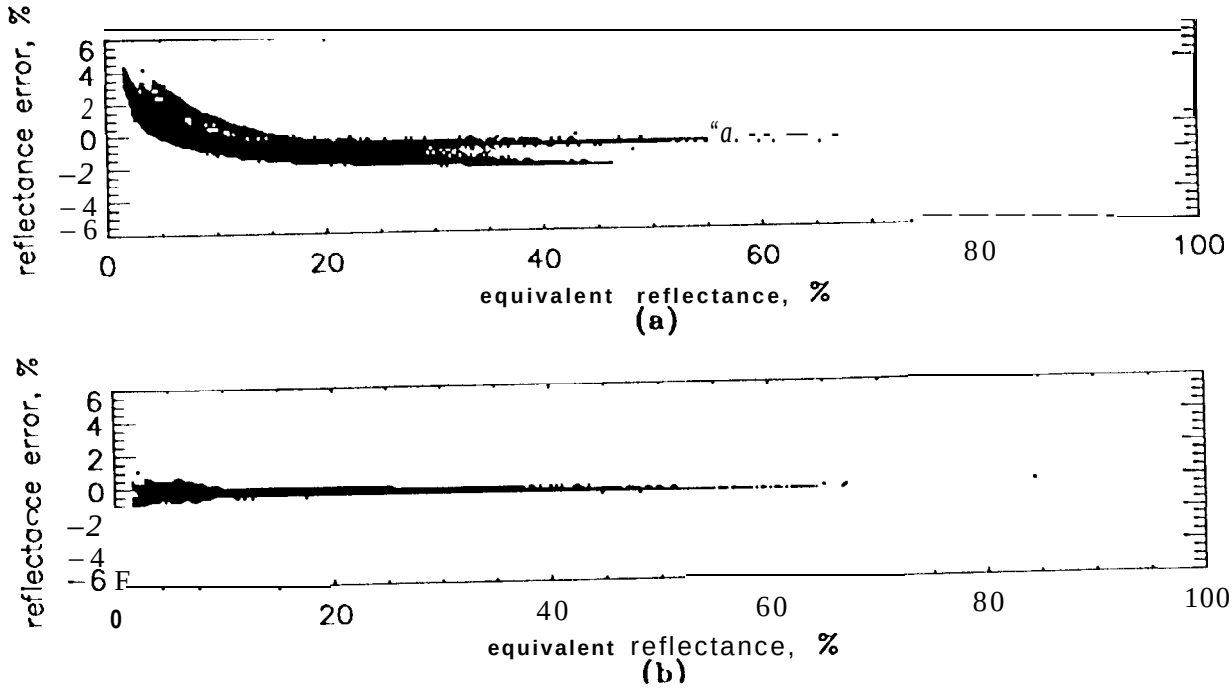

Figure 12. Band 4, errors in reflectance (a) without correction and (b) with out-of-band spectral correction.

4. CONCLUSIONS

The effect of the higher than desired out-of-band response of the MISR cameras ean be mitigated through a spectral out-of-band correction. This correction is done by using the other MISR bands to estimate the out-of-band radiance for a given observation. For this reason, the out-of-band correction cannot be done until the four MISR bands have been co-registered. For scenes with a high in-band equivalent reflectance and/or little spectral content, the correction is not needed. However, in the case of low in-band equivalent reflectance scenes the correction ean greatly reduce errors introduced by the out-of-band response of the MISR cameras. Implementation of this correction is to be applied only to those Level 2 processes that require it.

S. ACKNOWLEDGMENTS

We wish to thank Valerie Duval, Ghobad Saghri, Daniel Preston, and Barbara Gaitley for the MISR spectral calibration functions, Jessica Faust for the AVIRIS field panel data, and Thomas Chrien for the AVIRIS imagery. The work described in this paper was carried out by the Jet Propulsion Laboratory, California Institute of Technology, under a contract with the National Aeronautics and Space Administration.

6. REFERENCES

1. Korechoff, R.P, D.J. Diner, D.J. Preston, C.J. Bruegge (1995). In Advanced and Next-Generation Satellites. Spectroradiometer focal-plane design considerations: lessons learned from MISR camera testing. EUROPTO/ SPIE Vol. 2538, pp. 104-116, 25-28 September.

2. C. J. Bruegge, et al, "Level 1 Radiance Scaling and Conditioning Algorithm Theoretical Basis", JPL D- 11507, Rev. B

3. C. Wehrli, "Extraterrestrial Solar Spectrum", *World* Climate *Research Programme (WCRP) Publication Series No. 7,* WMO ITD-No. 149, pp 119-126, October 1986.

4. G. Vane, R. O. Green, et al, "The Airborne Visible/infrared Imaging Spectrometer (AVIRIS)", *Remote Sensing of Environment,* Volume 44, Numbers 2/3, pp.127-143, 1993.